Simultaneous stationarity and localization of linear wave packets: The importance of dimensionality and broad spectral support

G. Valiulis,[1,*] K. Kalantojus,[1] P. Di Trapani,[2] Y.-D Wang,[2,†] and O. Jedrkiewicz[3]
[1]*Department of Quantum Electronics, Vilnius University, Saulėtekio 9, Bldg. 3, LT-10222 Vilnius, Lithuania*
[2]*CNISM and Dipartimento di Fisica e Matematica, University of Insubria, Via Valleggio 11, 22100 Como, Italy*
[3]*Istituto di Fotonica e Nanotecnologie, CNR, Piazzale L. Da Vinci 32, Milano, Italy*
(Received 9 January 2014; published 8 May 2014)

In this paper we review the conditions needed for the localization and stationarity of a wave packet during propagation in a linear transparent medium. The requirements on the dimensionality and spatiotemporal frequency content for wave packets with such characteristics are discussed. In particular, we demonstrate how the localization of the stationary two-dimensional solution of the propagation equation depends on the features and shape of its spatiotemporal spectral bandwidth. The spatiotemporal properties of the one-dimensional (1D) spatial and 1D temporal beams stationarily propagating in dispersive materials are illustrated both in the normal and in the anomalous dispersion regime.

DOI: 10.1103/PhysRevA.89.053809 PACS number(s): 42.25.Bs, 42.65.Re

I. INTRODUCTION

The generation of localized stationary propagating optical wave packets is one of the most challenging tasks in nonlinear optics. Strongly localized (finite energy) wave packets stationary propagating in a nonlinear medium are known as solitary waves or solitons. The formation of these kinds of wave packets (WPs) requires specific conditions [1,2]. However, other types of (weakly) localized WPs exist thanks to their conical nature, and in the last few years stationary WPs propagating without diffraction and dispersion in linear or in nonlinear dispersive media have been the object of several studies [3–10]. Localized and quasistationary (with finite energy due to beam apodization) three-dimensional wave packets have been generated also in nonlinear processes [11–16], with asymptotic features relating to those of nondiffracting and nondispersive polychromatic Bessel beams in linear dispersive media. A description of conical waves in a linear medium has been given in [17] showing how these can be identified with X-shaped or O-shaped modes of the wave equation in media with, respectively, normal or anomalous group velocity dispersion (GVD). On the other hand, as we shall see in the present work, the study of the simultaneous properties of stationarity and localization of linear WPs deserves special care, and needs the understanding of the role of the dimensionality and spectral content of the wave packet.

In general the stationarity of a WP in a linear dispersive medium requires the infinite energy to be distributed in space and time, in order to ensure constant propagation conditions along an infinite path. Some examples of stationary waves in a linear medium are well known: the monochromatic plane wave, which is existing as an unbounded object in the three-dimensional space, but is characterized by a single wave vector ($\vec{k}$), and thus can be treated as a one-dimensional (1D) entity; the monochromatic Bessel beam (BB), which also has infinite energy and due to its conical nature is a stationary propagating two-dimensional (2D) object. A similar stationary propagating WP is the two-dimensional spatiotemporal Bessel beam (STBB), also featured by infinite energy [18]. Analogously, the three-dimensional X waves and O waves are stationary wave packets in linear media when having unlimited energy [3–6,8,9]. All the mentioned examples, except for the monochromatic plane wave (which is not a localized wave packet neither in time nor in space) are WPs which are localized at least in two dimensions. In order to be localized in one dimension (spatial or temporal), the WP should be featured by a spectral bandwidth with different components (in accordance with the Fourier transform properties). Note that in a nonlinear medium the 1D localization still requires nonmonochromaticity, but a WP with such characteristics can be stationary due to the "external force" produced by nonlinearity via nonlinear phase shift. This leads to the generation of the so-called solitons [1]. In contrast, in a linear medium, a polychromatic one-dimensional wave packet is nonstationary due to dispersion (or diffraction).

It turns out, as preliminarily shown in [19] where we mainly focused on the spatial aspect of the beam localization, that the simultaneous features of wave stationarity and localization in a linear medium requires infinite energy, a broad polychromatic spectral support, and at least two dimensions. The last point is supported by the existence, as mentioned before, of the 2D spatially localized BB, or of the 2D STBB characterized in [18], both stationary in propagation. In both cases, the ringlike spatial spectrum of the BB or the ringlike spatiotemporal spectrum of the STBB leads to a Bessel profile in the near field, and to its localization in space and in space-time, respectively.

The aim of the present paper is to discuss and review in detail the necessary requirements on the spatiotemporal frequency content of a two-dimensional wave packet (1D in space and 1D in time), so that it can be simultaneously stationary *and* localized when propagating in a linear medium, both in the normal and in the anomalous dispersion regime; this is respectively the case, for instance, of the two-dimensional counterpart of the 3D X wave, stationary in the normal dispersion regime and briefly illustrated in [19], and of the STBB, the latter being the two-dimensional space-time version of the 3D so-called O wave, stationary in the anomalous

*gintaras.valiulis@ff.vu.lt
†Present address: Nanyang Technological University, School of Mechanical and Aerospace Engineering, Singapore.

dispersion regime. The spatial and temporal characteristics of the localization of the stationary two-dimensional solution of the propagation equation deserve a thorough study, and we shall demonstrate in both group velocity dispersion regimes how these depend on the features of the wave packet spatiotemporal spectral support.

In Sec. II we present the extended theoretical model where the two-dimensional field solution of the linear propagation equation is derived together with its spatiotemporal spectrum dependence, and the conditions for stationarity and localization are discussed. The spatiotemporal features of the 2D wave packet stationarily propagating in a linear medium are presented in Sec. III, concentrating on the anomalous dispersion regime in Sec. III A and on the normal dispersion regime in Sec. III B. The spatial and temporal intensity profiles of the radiation are discussed together with the realistic case of finite energy (beam apodization). In Sec. IV the conclusions are presented.

II. TWO-DIMENSIONAL SOLUTION OF THE LINEAR WAVE EQUATION

The propagation of the linearly polarized light wave in linear transparent media is described by the scalar wave equation

$$\Delta E - \frac{1}{c^2}\frac{\partial^2 D}{\partial t^2} = 0, \tag{1}$$

where $E(t,r)$ is the electric field, $D(t,r)$ is the electric displacement, c is the speed of light, t is time, $r=(x,y,z)$ are the coordinates, and $\Delta = \frac{\partial^2}{\partial x^2}+\frac{\partial^2}{\partial y^2}+\frac{\partial^2}{\partial z^2}$ is the Laplace operator. In an isotropic dispersive medium the electric displacement $D(t,r)$ reads as

$$D(t,r) = \int_0^\infty \epsilon(t')E(t-t',r)dt', \tag{2}$$

where $\epsilon(t)$ is the linear response function [$\epsilon(t)=0$ when $t<0$] related to linear permittivity $\epsilon(\omega)$ via the Fourier transform:

$$\epsilon(\omega) = \int_0^\infty \epsilon(t)e^{-i\omega t}dt. \tag{3}$$

By means of the Fourier transform it is possible to write down a solution of the wave equation (1) in the full 3D case, but we shall focus here on the two-dimensional solution, i.e., a WP modulated in time t and featured by one transverse coordinate x, propagating along the z axis. In the coordinate frame moving with the velocity u_0 and setting $\eta = t-\frac{z}{u_0}$, the electric field of such a wave is

$$E(t,x,z) = A(\eta,x,z)\exp\{i(\omega_0 t - k_0 z)\} + \text{c.c.}, \tag{4}$$

where the complex amplitude $A(\eta,x,z)$ reads as

$$A(\eta,x,z) = \frac{1}{(2\pi)^2}\iint_{-\infty}^{\infty} S_0(\Omega,k_x) \times \exp\{i[\Omega\eta - k_x x - G(\Omega,k_x)z]\}d\Omega\, dk_x, \tag{5}$$

where $\Omega=\omega-\omega_0$ (ω_0 being the carrier frequency). $S_0(\Omega,k_x)$ is the initial spatiotemporal spectrum of the WP and c.c. denotes the "complex conjugated" term. The effect of material dispersion and diffraction is described by

$$G(\Omega,k_x) = \sqrt{k^2(\omega_0+\Omega)-k_x^2} - \left(k_0 + \frac{\Omega}{u_0}\right), \tag{6}$$

where $k(\omega_0+\Omega)$ is the dispersion relation function depending on the material properties [$k(\omega)=\frac{\omega n(\omega)}{c}$], and $k_0=k(\omega_0)$. Note, that the freedom in choosing an initial spectrum $S_0(\omega,k_x)$ reflects in the freedom in defining ω_0. Commonly, it can be treated as a central (carrier) frequency and defined, for example, as the "center of mass" of the wave packet:

$$\omega_0 = \frac{\int \omega|S_0(\omega,k_x)|^2 d\omega\, dk_x}{\int |S_0(\omega,k_x)|^2 d\omega\, dk_x}. \tag{7}$$

Equations (5) and (6) describe the unidirectional solution of the linear wave equation in the nonparaxial case when accounting for the full dispersion [$k(\omega)$] of the material. On the other hand, by using Taylor expansion $k(\omega_0+\Omega)=k_0+\frac{\Omega}{u}+\frac{1}{2}g\Omega^2+\cdots$ and assuming a paraxial beam ($k_x^2 \ll k_0^2$), we obtain from Eq. (6),

$$G(\Omega,k_x) = \nu\Omega + \frac{1}{2}g\Omega^2 - \frac{k_x^2}{2k_0}, \tag{8}$$

where $\nu = u^{-1}-u_0^{-1}$ is the group velocity mismatch, u is the "material" group velocity $u=(\frac{dk}{d\omega})^{-1}|_{\omega=\omega_0}$, and $g=\frac{d^2k}{d\omega^2}|_{\omega=\omega_0}$ is the group velocity dispersion coefficient. Thus Eq. (5) together with Eq. (8) describe the solution of the "paraxial" parabolic equation for the wave envelope, which can be written as

$$\frac{\partial A}{\partial z} + \nu\frac{\partial A}{\partial \eta} - \frac{i}{2}g\frac{\partial^2 A}{\partial \eta^2} + \frac{i}{2k_0}\frac{\partial^2 A}{\partial x^2} = 0. \tag{9}$$

In the following we shall discuss the possibilities to obtain a stationary propagating 2D localized WP. Note that Eq. (5) describes the solution of the wave equation with any initial spatiotemporal spectrum $S_0(\Omega,k_x)$. In general, the WP stationarity requires the function $G(\Omega,k_x)$ to be linear [3] of the form $G(\Omega,k_x)=\gamma_1\Omega+\gamma_2 k_x+\gamma$, where γ_1, γ_2, and γ are free parameters, so that the field amplitude profile can be written as $A(\eta,x,z)=A_0(\eta-\gamma_1 z, x-\gamma_2 z)\exp(-i\gamma z)$; thus using Eq. (6) the following relation must be satisfied:

$$\sqrt{k^2(\omega_0+\Omega)-k_x^2} = k_0+\gamma+\Omega\left(\gamma_1+u_0^{-1}\right)+\gamma_2 k_x. \tag{10}$$

As already discussed in [19], in order for a WP to have a spatially localized and stationary profile in one spatial dimension, it has to be a nonmonochromatic solution, thus with some temporal spectral bandwidth. From Fourier transform properties we know that the finite dimensions of the WP implies having a bandwidth. Moreover, the stationarity condition expressed by Eq. (10) shows that the spatial localization and the temporal localization are not independent, since it sets $\Omega=f(k_x)$. As a consequence, spatial localization, which implies having a bandwidth of spatial frequencies, necessarily implies having a bandwidth of temporal frequencies as well. Thus a 2D linear WP (1D spatial and 1D temporal) can be stationary propagating *and* localized when its space and time coordinates become entangled via angular dispersion, i.e., when the different temporal frequencies are distributed at different propagating angles. Such a wave packet can be described in the temporal-frequency domain by setting the spatiotemporal spectrum $S_0(\Omega,k_x) = 2\pi S_0(\Omega)\delta(k_x - \Delta(\Omega))$, or in the spatial-frequency domain by setting $S_0(\Omega,k_x) = 2\pi S_0(k_x)\delta(\Omega - \Delta(k_x))$. We shall consider from now on the first case, where the function $\Delta(\Omega)$ defines the transverse wave vector $k_x = k\sin[\theta(\Omega)] = \Delta(\Omega)$ dependence on frequency, and consequently defines the angular dispersion $\theta(\Omega)$ of the WP.

We shall now derive the spectral dependence of the field amplitude stationary solution satisfying the wave equation. We start by rewriting Eq. (5) in the following way:

$$A(\eta,x,z) = \frac{1}{2\pi}\int_{-\infty}^{\infty} S_0(\Omega)\exp\{i[\Omega\eta - \Delta(\Omega)x - G(\Omega,\Delta(\Omega))z]\}d\Omega. \tag{11}$$

In general, the solution, Eq. (11), describes a nonstationary wave with angular dispersion. In order to guarantee stationarity we should set the angular dispersion $[\Delta(\Omega)]$ such that it can support the wave invariant propagation condition

$$G(\Omega,\Delta(\Omega)) = \alpha\Omega + \beta, \tag{12}$$

where α and β are free parameters. Indeed for the longitudinal wave vector $k_z = \sqrt{k^2(\omega_0+\Omega) - k_x^2}$, from Eqs. (6) and (12) we have $k_z(\Omega) = k(\Omega)\cos[\theta(\Omega)] = k_0 + \beta + \Omega(\alpha + u_0^{-1})$. The linear dependence on frequency guarantees the stationary propagation. From Eqs. (6) and (12) we can also derive

$$\Delta(\Omega) = \pm\sqrt{k^2(\omega_0+\Omega) - \left[k_0 + \beta + \Omega\left(\frac{1}{u_0} + \alpha\right)\right]^2}, \tag{13}$$

where the two possible signs represent the two symmetric branches of the angular dispersion. In order to have a WP symmetric across the x axis we should consider both branches of the spectrum [the material is linear and a linear superposition of the WPs (11) is possible]. Thus in Eq. (5) we substitute the initial spectrum distribution, which accounts for both branches of the angular dispersion, and we obtain

$$A(\eta,x,z) = \int_{-\infty}^{\infty} S_0(\Omega)\cos[\Delta(\Omega)x] \times \exp\{i[\Omega\eta - (\alpha\Omega+\beta)z]\}\frac{d\Omega}{2\pi}, \tag{14}$$

or in (t,x) frame,

$$A(t,x,z) = e^{-i\beta z}\int_{-\infty}^{\infty} S_0(\Omega)\cos[\Delta(\Omega)x] \times \exp\left\{i\Omega\left[t - z\left(\frac{1}{u_0}+\alpha\right)\right]\right\}\frac{d\Omega}{2\pi}. \tag{15}$$

Since the electric field is derived by multiplying the complex amplitude by the carrier exponent $e^{i(\omega_0 t - k_0 z)}$, it is obvious that Eq. (15) describes the stationary propagating WP with group velocity $u_{\mathrm{gr}} = \frac{1}{u_0^{-1}+\alpha}$ and phase velocity $v_{\mathrm{ph}} = \frac{\omega_0}{k_0+\beta}$. The transverse wave vector is defined by $\Delta(\Omega)$ $[k_x = \Delta(\Omega)]$ and the longitudinal wave vector is $k_z = \sqrt{k^2 - k_x^2} = k_0 + \beta + \Omega(1/u_{\mathrm{gr}})$. We note for completeness that in the regime of paraxial approximation, instead of writing the spectral dependence of the transverse wave vector as Eq. (13), by combining Eq. (8) with the condition, Eq. (12), we have

$$\Delta(\Omega) = \pm\sqrt{k_0[g\Omega^2 + 2(\nu-\alpha)\Omega - 2\beta]}, \tag{16}$$

and in this case Eq. (14) describes the solution of the paraxial equation, Eq. (9). From now on we shall keep the paraxial approximation, and for simplicity we shall choose the coordinate system moving with the WP group velocity in the material $u_0 = u\ (\nu = 0)$.

III. SPACE-TIME FEATURES OF THE STATIONARY 2D LOCALIZED WAVE PACKET

A. Wave packet spectral support

As the spatial and temporal features of the stationary wave packet depend on its spatiotemporal spectral support, it is important to briefly describe the parameters entering into play in the spectral bandwidth shape. Note that these can be chosen with some freedom: The carrier frequency ω_0 and the spectrum profile $S_0(\Omega)$ can be defined independently [we can define ω_0 and introduce some frequency shift for the $S_0(\Omega)$ profile]. This gives the possibility to introduce a frequency offset $\Omega_0 = \frac{\alpha}{g}$ and to describe the angular dispersion by just one free parameter which we shall denote by $\widetilde{\beta}$. The second parameter (α) is predefined by choosing the shift of the $S_0(\Omega)$ profile with respect to Ω_0. Therefore, Eq. (16) can also be written as

$$\Delta(\Omega) = \pm\sqrt{k_0[g\widetilde{\Omega}^2 - \widetilde{\beta}]}, \tag{17}$$

where $\widetilde{\beta} = 2\beta + \frac{\alpha^2}{g}$ and $\widetilde{\Omega} = \Omega - \Omega_0$. In this way we have a unified representation for any angular dispersion curve, depending just on one parameter $\widetilde{\beta}$. Since the function $k'(\omega_0 + \Omega_0) = k'(\omega_0) + g\Omega_0$ for the new "central" frequency $\widetilde{\Omega} = 0$, the group velocity value is $u_{\mathrm{gr}} = \frac{1}{u^{-1}+\alpha}$. Figure 1 illustrates possible angular dispersion supports $k_x = \Delta(\Omega)$ in different group velocity dispersion regimes, with the superimposed freely chosen spectrum $S_0(\Omega)$.

B. Anomalous GVD case ($g < 0$)

The transparent dielectric medium in the near infrared spectral region usually possesses the anomalous group velocity dispersion features. In such case ($g < 0$) the stationary solution exists only for $\widetilde{\beta} < 0$ and the angular dispersion curve

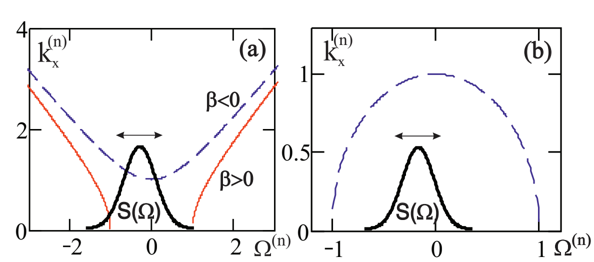

FIG. 1. (Color online) Angular dispersion support: (a) normal GVD case ($g > 0$); (b) anomalous GVD ($g < 0$). Black solid line depicts the $S_0(\Omega)$. Temporal and spatial frequencies are normalized as $\Omega^{(n)} = \Omega\sqrt{|g|/|\widetilde{\beta}|}$ and $k_x^{(n)} = k_x/\sqrt{k_0|\widetilde{\beta}|}$.

becomes O shaped [see Fig. 1(b)]. Since $g < 0$ and $\widetilde{\beta} < 0$ we can introduce the more convenient parameters $\Gamma^2 = -k_0\widetilde{\beta}$, $\gamma^2 = k_0|g|$. Thus in this case, we have $\Delta(\Omega) = \sqrt{\Gamma^2 - \gamma^2\Omega^2}$, where for simplicity of notation $\widetilde{\Omega}$ has been replaced by the symbol Ω. The infinite integration margins in Eq. (15) lead to a delocalized wave with exponentially growing tales. The localized 2D solution is possible when $\Delta(\Omega)$ is a real number, therefore the wave packet should contain frequency components within a finite range, i.e., the integration margins should be set from $-\frac{\Gamma}{\gamma}$ to $\frac{\Gamma}{\gamma}$:

$$A(t,x,z) = e^{-i\beta z}\int_{-\Gamma/\gamma}^{\Gamma/\gamma} S_0(\Omega)\cos[(\Delta(\Omega)x)] \times \exp\{i\Omega[t - z/u_{\rm gr}]\}\frac{d\Omega}{2\pi}. \quad (18)$$

In the case where $S_0(\Omega) = \frac{a_0}{\sqrt{\Gamma^2-\gamma^2\Omega^2}}$ we have after integration

$$A(t,x,z) = \frac{a_0 e^{i(\Omega_0\tau-\beta z)}}{\gamma} J_0\left(\sqrt{\frac{\Gamma^2}{\gamma^2}\tau^2 + \Gamma^2 x^2}\right). \quad (19)$$

Here $\tau = t - \frac{z}{u_{\rm gr}}$, $u_{\rm gr} = \frac{1}{u^{-1}+\alpha}$. This is the field amplitude of the spatiotemporal Bessel beam, whose spatiotemporal intensity profile is shown in Fig. 2, and which has already been observed and characterized in [18]. This wave packet is analogous to a 2D version of the so-called O wave stationary in the anomalous GVD regime [17]. As described in [18], for the experimental realization of such a WP, by means of a pulse shaper setup, the ring-shaped spectral mask should be uniformly illuminated (this corresponds to a constant intensity spatiotemporal spectrum, leading thus to a localized Bessel spatiotemporal profile). However the on-axis spectrum $S_0(\Omega) = \frac{a_0}{\sqrt{\Gamma^2-\gamma^2\Omega^2}}$, leading to the ideal Bessel profile both in space and time, contains two infinite spikes separated by some background (as shown in the top right part of Fig. 2).

Different stationary wave packets could be formed by using other shapes of the spectrum. If $S_0(\Omega) = \text{const}$, $(|\Omega| < \Gamma/\gamma)$ is a simple rectangular on-axis spectral profile (no spikes) the resulting WP is the incomplete STBB illustrated in Fig. 3; however, a double-spiked spectrum (without background) corresponds to an X-shaped array of pulses (leading to a 1D array of spatially localized time-integrated beams), which

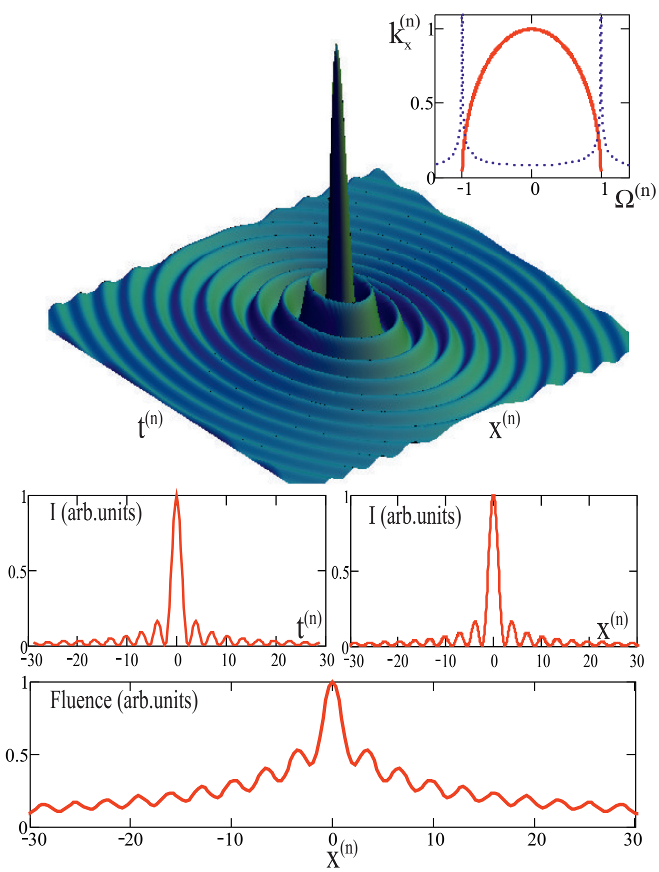

FIG. 2. (Color online) Intensity profile of spatiotemporal Bessel beam solution for the anomalous GVD case. Below are shown the 1D temporal and spatial profiles, and the time-integrated profile (bottom row). The angular dispersion support is shown in the top right corner inset; the dashed line represents the $|S_0(\Omega)|$. Normalized units are used: $\Omega^{(n)} = \Omega\sqrt{|g|/|\widetilde{\beta}|}$, $k_x^{(n)} = k_x/\sqrt{k_0|\widetilde{\beta}|}$, $t^{(n)} = t\sqrt{|\widetilde{\beta}|/|g|}$, $x^{(n)} = x\sqrt{k_0|\widetilde{\beta}|}$.

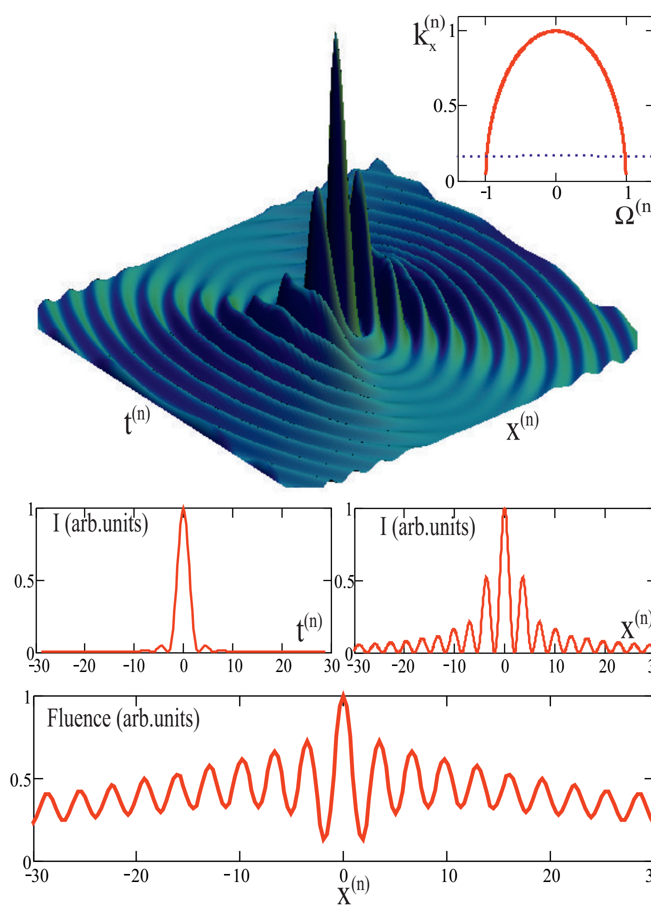

FIG. 3. (Color online) Intensity profile of the *incomplete* spatiotemporal Bessel beam in the anomalous GVD region. Shown below are the 1D temporal and spatial profiles, and the time-integrated profile (bottom row). The angular dispersion support is shown in the top right corner inset; the dashed line represents the $|S_0(\Omega)|$. Units are normalized as in Fig. 2.

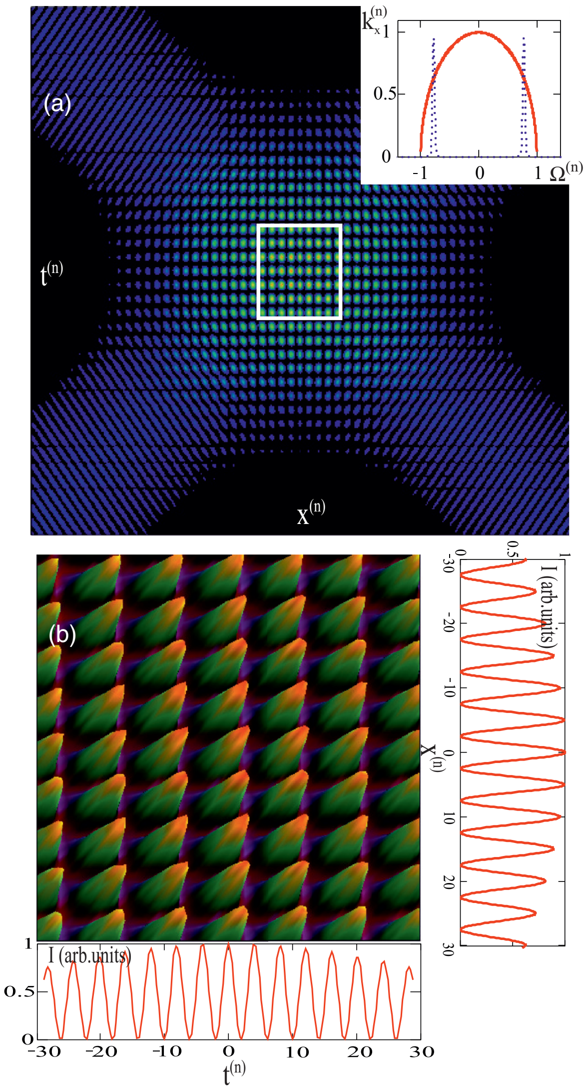

FIG. 4. (Color online) (a) X-shaped array of pulses in the anomalous group velocity dispersion region. The angular dispersion support is shown in the top right corner inset; the dashed line represents the $|S_0(\Omega)|$. Units are normalized as in Fig. 2. (b) Zoomed rectangular area with 1D temporal and spatial intensity profiles.

may be of interest in all those applications where pixel-like localized light sources are needed (for instance, in arrays and matrices scribing of transparent materials) (Fig. 4). In all these cases the resulting WPs are stationary. The invariance during propagation is guaranteed by the infinite energy of the solution. In fact the spatiotemporal localization of STBB is obvious because of the ring-shaped spatiotemporal spectral support. Also note that if one increases the thickness of this ring-shaped spectrum, one gets instead of the ideal STBB, the spatiotemporal Bessel Gaussian wave packet, quasistationary in materials with anomalous dispersion regime.

We highlight that the polychromatic spectral support is clearly important for having a precise single peak location of the WP. This is evident in the spatial and temporal sections of the intensity profiles reported in Figs. 2 and 3. On the other hand, if we concentrate only on the spatial aspect of the 1D localization and consider the time-integrated profile of the beam (whose contrast features are essential, for instance, for an effective radiation absorption and thus energy to matter transfer in microfabrication applications), we note that the most enhanced central peak in the beam appears only in the case of Fig. 2, thus thanks to the presence of a broad spectral bandwidth but containing the two on-axis frequency peaks.

It should be mentioned, that there are some limitations for creating stationary spatiotemporal Bessel beams with very narrow spatial profile. These come from the relation between the STBB pulse duration τ_s and the beam diameter d_s. This relation can be derived from the solution given by Eq. (19) and reads as $\tau_s/\tau_0 = d_s/d_0\sqrt{(L_d/L_g)}$, where $L_d = \frac{1}{2}k_0 d_0^2$ is the diffraction length (beam confocal parameter) calculated for a diameter d_0 of a Gaussian beam and $L_g = \frac{\tau_0^2}{2g}$ is the group velocity dispersion length calculated for a duration τ_0 of the Gaussian pulse. For instance in fused silica, and for a 2 μm wavelength radiation, we obtain a 10 μm beam diameter provided the pulse duration is 7 fs, this being roughly the optical cycle (6.6 fs) at 2 μm. Therefore it turns out that the minimum achievable diameter of such a localized beam should be 20–30 μm. More tiny 1D spatial beams could be generated at shorter wavelengths, but in that case the GVD becomes normal.

C. Normal GVD case ($g > 0$)

In the normal GVD region the angular dispersion support $\Delta(\Omega) = \pm\sqrt{k_0[g\widetilde{\Omega}^2 - \widetilde{\beta}]}$ becomes X shaped, as shown in Fig. 1(a). It is possible to have a stationary solution of the linear propagation equation in both cases where $\widetilde{\beta} < 0$ (spectral gap in the transverse k-vector space) and $\widetilde{\beta} > 0$ (spectral gap in the temporal-frequency space). We will concentrate on the first case, keeping in mind that the second one could be identically analyzed, because of the space-time analogy (temporal variable t can be exchanged with the spatial one, x).

The spatiotemporal localization of the wave packet is not so obvious as in the anomalous GVD case where the Bessel profile clearly appears due to the ring-shaped spatiotemporal spectrum. In order to analyze the formation of stationary and localized wave packets in a normally dispersive material, we can perform the integration in Eq. (15) for different cases. We shall illustrate the localization features of the resulting space-time intensity profile of a stationary (1D spatial, 1D temporal) wave packet. The case without spatial gap in the spectral distribution is shown in Fig. 5 [$\beta = 0$ in the top right corner inset: the solid line is $k_x = \Delta(\Omega)$, while $S_0(\Omega)$ is shown by dashes)]. The WP has a sharp peak, but the tails are constant and nondecaying, as also shown in the spatial and temporal sections of Fig. 5.

We should also note, that in contrast to the 2D spatial case, the introduction of a gap in the spatiotemporal spectrum ($\beta < 0$) is here a necessary condition for having a decay in the tails of the spatial intensity profile (Fig. 6). This can be shown analytically by analyzing the asymptotic behavior of Eq. (15). In order to demonstrate the gap influence on the tails asymptotic features we considered the solution given by Eq. (15) at a given distance z (since it is invariant with propagation we can take $z = 0$), and an angular dispersion

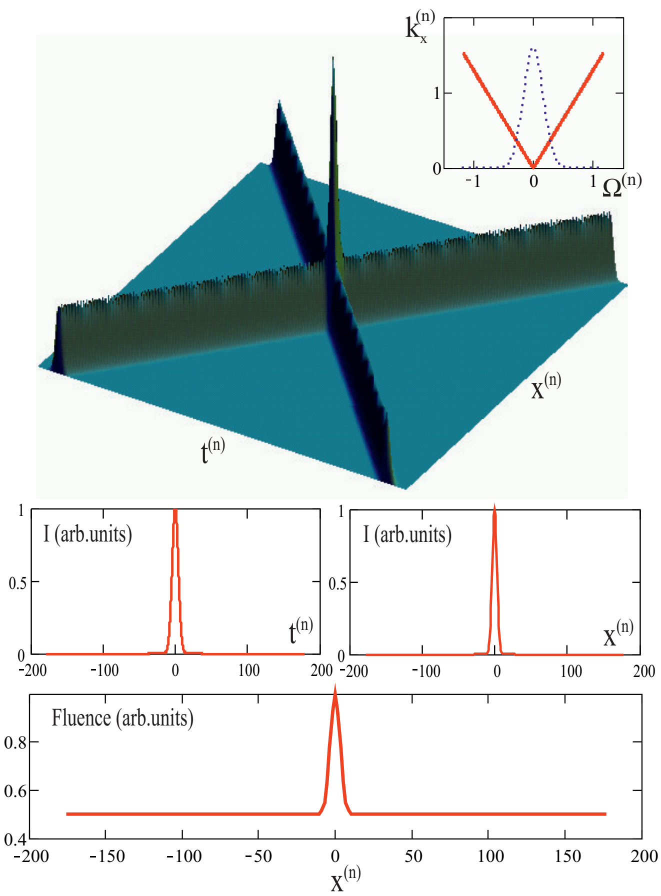

FIG. 5. (Color online) Intensity profile of the 2D stationary solution of the wave equation featured by normal dispersion spectral support $[k_x = \Delta(\Omega)]$ *without* angular frequency gap $(\widetilde{\beta} = 0)$ as shown in the top right corner inset; the dashed line represents the $|S_0(\Omega)|$. Below are shown the 1D temporal and spatial profiles, and in the bottom row the time-integrated profile. Units are normalized: $\Omega^{(n)} = \Omega\sqrt{g/k_0}$, $k_x^{(n)} = k_x/k_0$, $t^{(n)} = t\sqrt{k_0/|g|}$, $x^{(n)} = xk_0$.

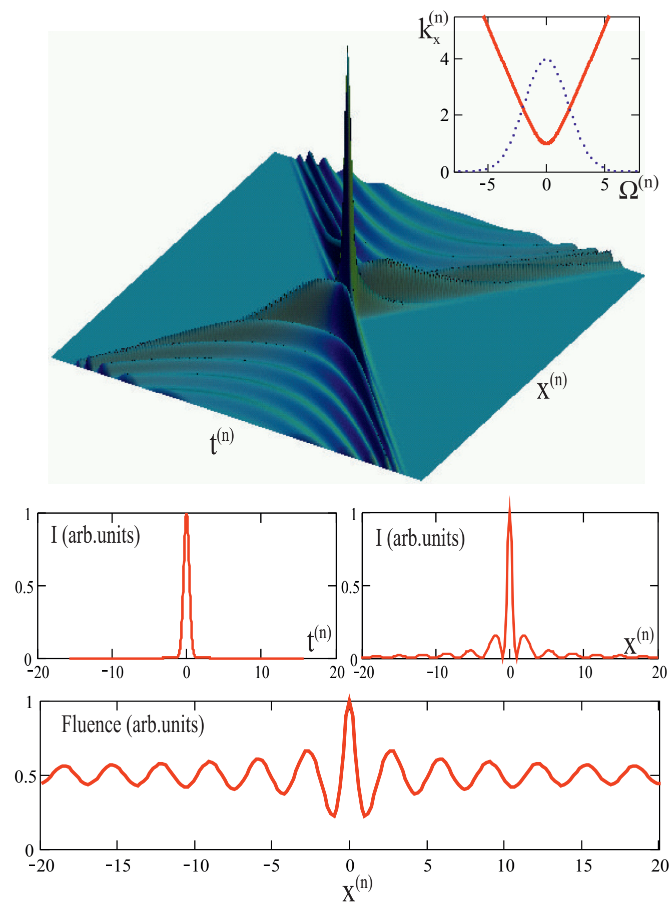

FIG. 6. (Color online) Intensity profile of the 2D stationary solution of the wave equation featured by normal dispersion spectral support $[k_x = \Delta(\Omega)]$ *with* angular frequency gap as shown in the top right corner inset; the dashed line represents the $|S_0(\Omega)|$. Units are normalized as in Fig. 2. 1D temporal and spatial profiles (below), and time-integrated profile (bottom row).

described by $\Delta(\Omega) = \sqrt{k_0(g\Omega^2 - 2\beta)}$ $(\alpha = 0, \beta < 0)$. The "characteristic" coordinates along the X-shaped tails could be introduced: $\xi = t - x\sqrt{k_0 g}$ and $\zeta = t + x\sqrt{k_0 g}$. If $\beta = 0$, we obtain from Eq. (15) $A(\xi,\zeta) = A_0(\xi) + A_0(\zeta)$, with $A_0(t) = \frac{1}{2\pi}\int_{-\infty}^{\infty} S_0(\Omega)\exp(i\Omega t)d\Omega$ being the temporal WP profile corresponding to an initial spectrum $S_0(\Omega)$. The solution $A(\xi,\zeta)$ represents nothing more than the superposition of two tilted wave packets in the space-time plane. If we consider one of the two tails (for instance $\zeta = 0$, $\xi \neq 0$) we have $A(\xi,0) = A_0(\xi) + A_0(0)$. For a spectrum $S_0(\Omega)$ related to any "bell-shaped" pulse profile featured by the asymptotic behavior $A_0(t)|_{|t|\to\infty} = 0$, we obtain a WP characterized by a central spike of amplitude $A(0,0) = 2A_0(0)$, however, $A(\xi,0)|_{|\xi|\to\infty} = A_0(0) = \text{const}$, i.e., the tail is not decaying. This result is in accordance with the amplitude profile features obtained by integration of Eq. (15), as also shown in the corresponding intensity profile presented in Fig. 5. In contrast, a spatiotemporal spectrum with the presence of a gap between the two hyperbolic branches $(\beta < 0)$ leads to an X-shaped WP with decaying tails. This can be shown analytically by taking a rectangular spectrum $S_0(\Omega)|_{|\Omega|<a} = S_{00}$, $S_0(\Omega)|_{|\Omega|>a} = 0$. In this case from Eq. (15) we obtain

$$A(\xi,0) = \frac{S_{00}\mu}{\pi\xi\sigma^2}\left[(\mu + a)\sin\left(\frac{\xi(a-\mu)}{2}\right) + (\mu - a)\sin\left(\frac{\xi(a+\mu)}{2}\right)\right], \tag{20}$$

where $\mu = \sqrt{a^2 + \sigma^2}$, $\sigma^2 = -2\beta/g$.

From Eq. (20) we can see how the tail of the 2D X-type wave packet is in this case decaying as $A(\xi,0) \sim \frac{1}{\xi}$. The numerical integration of Eq. (15) also revealed that in the case of a Gaussian spectrum $S_0(\Omega)$ (with the same width as the rectangular spectrum considered for the result given above), the tails decay occurs even faster. Note, however, that in both cases illustrated in Figs. 5 and 6, the infinite energy of the theoretical solution supports the nondecaying tails in the time-integrated intensity profiles, shown just below the space-time profiles.

The important role of polychromaticity in the 1D spatial localization is confirmed by the result of Fig. 7, obtained for a WP angular dispersion identical to that of Fig. 6, but with a temporal bandwidth ten times smaller. In that case

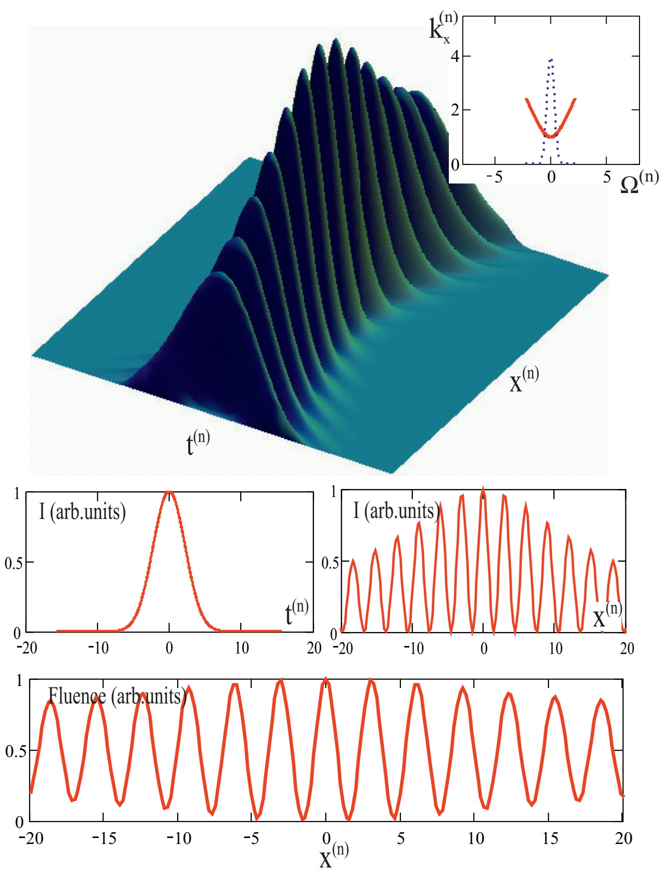

FIG. 7. (Color online) Intensity profile of the 2D stationary solution of the wave equation featured by *narrow spectrum* and normal dispersion spectral support $[k_x = \Delta(\Omega)]$ with angular frequency gap as shown in the top right corner inset; the dashed line represents the $|S_0(\Omega)|$. Units are normalized as in Fig. 2. 1D temporal and spatial profiles (below), and time-integrated profile (bottom row).

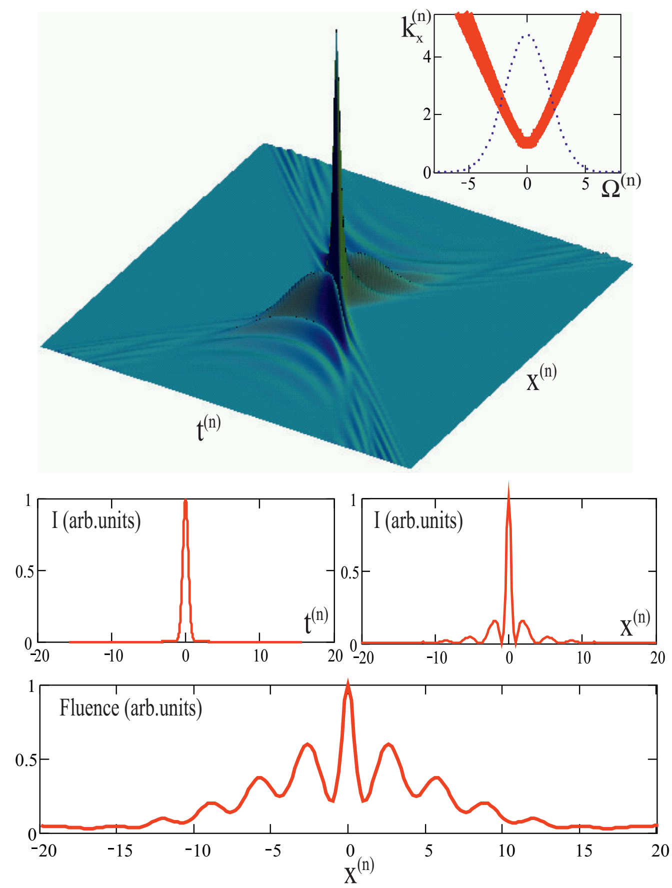

FIG. 8. (Color online) Intensity profile of the 2D stationary solution of the wave equation featured by *thick* normal dispersion spectral support $[k_x = \Delta(\Omega)]$ with angular frequency gap shown in the top right corner inset; the dashed line represents the $|S_0(\Omega)|$. Units are normalized as in Fig. 2. 1D temporal and spatial profiles (below), and time-integrated profile (bottom row).

an oscillating spatial profile [due to the cosine function in Eq. (15)] appears, and the spatial localization vanishes. Figure 8 shows the effect of the angular dispersion line $[k_x = \Delta(\Omega)]$ "thickness" which acts as a beam apodization effect, thus leading to a time-integrated profile with decaying tails (in this case the solution is energy limited and thus quasistationary).

Also in this case, the spatial and temporal localization features are not independent, and the relation between pulse duration and central spike diameter $[\tau_s/\tau_0 = d_s/d_0\sqrt{(L_d/L_g)}]$ is still valid. Nevertheless since the normal group velocity dispersion regime is typical for radiation in the visible and UV spectral region where the optical cycle is very small, the localization limits are tighter than in the anomalous dispersion regime. For instance, in a BBO crystal a stationary localized wave packet at 300 nm wavelength (corresponding to 1 fs optical cycle) could have a 2 μm beam diameter provided the pulse duration is 7.5 fs.

IV. CONCLUSIONS

To conclude, in this paper we have reviewed the conditions needed for the localization and stationarity of a wave packet during propagation in a linear transparent medium, highlighting the requirements on its dimensionality and its spatiotemporal frequency content. The results presented support the concept that at least two dimensions (where space and time are equivalent) are needed in order to have simultaneous stationarity and localization of a WP. We have studied, in particular, the two-dimensional field solution of the linear propagation equation, which has been derived together with its spatiotemporal spectrum dependence, and we have discussed the conditions for stationarity and localization of such a 2D wave packet in the normal and anomalous group velocity dispersion regimes. The theoretical model highlights that a 2D (1D spatial and 1D temporal) stationary WP in a linear dispersive medium can also be sharply localized (in both dimensions x and t) provided that its spectrum is featured by spatial and temporal coordinates entangled via angular dispersion. The importance of the temporal polychromaticity of the WP bandwidth has been put in evidence, both for the case of localized 2D X-type waves (2D counterpart of the X waves) propagating stationarily in the normal dispersion regime, and for the case of localized spatiotemporal Bessel beams or even spatiotemporal localized "pixel-like" wave packets stationarily propagating in the anomalous dispersion regime. From the spatial point of view, in order to have high contrast temporally integrated beam profiles, we have noticed that in the positive GVD case, the beam apodization plays an important role reflecting in the necessity of a finite width of the spatial bandwidth supporting the spectrum of the resulting quasistationary wave packet. The aim of our work was to present a unified and systematic theoretical description of different 2D wave packet configurations both spatiotemporally localized and stationary, showing also how these strongly depend on the features and shape of their spatiotemporal spectral support. Finally note that the results obtained here suggest that the entanglement between the spectral-spatial and spectral-temporal coordinates could be exploited even more generally, targeting for instance, different spatiotemporal profiles outcomes for applications where tailored features of the pulse and beam, as the amplitude profile, the localization, and the stationarity, can be controlled along propagation.

ACKNOWLEDGMENTS

G. Valiulis and K. Kalantojus acknowledge Grant No. VP1-3.1-ŠMM-07-K-03-001 from the Lithuanian Science Council.

[1] A. Buryak, P. Di Trapani, D. Skryabin, and S. Trillo, Phys. Rep. **370**, 63 (2002).
[2] J. S. Aitchison and G. I. Stegeman, Opt. Quantum Electron. **30**, 501 (1998), special issue on spatial solitons.
[3] H. Sonajalg and P. Saari, Opt. Lett. **21**, 1162 (1996).
[4] H. Sonajalg, M. Ratsep, and P. Saari, Opt. Lett. **22**, 310 (1997).
[5] M. A. Porras, Opt. Lett. **26**, 1364 (2001).
[6] M. A. Porras, R. Borghi, and M. Santarsiero, Opt. Commun. **206**, 235 (2002).
[7] S. Orlov, A. Piskarskas, and A. Stabinis, Opt. Lett. **27**, 2167 (2002); **27**, 2103 (2002).
[8] M. A. Porras, S. Trillo, and C. Conti, Opt. Lett. **28**, 1090 (2003).
[9] M. A. Porras, G. Valiulis, and P. Di Trapani, Phys. Rev. E **68**, 016613 (2003).
[10] D. N. Christodoulides, N. K. Efremidis, P. Di Trapani, and B. A. Malomed, Opt. Lett. **29**, 1446 (2004).
[11] P. Di, G. Valiulis, A. Piskarskas, O. Jedrkiewicz, J. Trull, C. Conti, and S. Trillo, Phys. Rev. Lett. **91**, 093904 (2003).
[12] M. Kolesik, E. M. Wright, and J. V. Moloney, Phys. Rev. Lett. **92**, 253901 (2004).
[13] D. Faccio, M. A. Porras, A. Dubietis, F. Bragheri, A. Couairon, and P. Di Trapani, Phys. Rev. Lett. **96**, 193901 (2006).
[14] P. Polesana, A. Couairon, D. Faccio, A. Parola, M. A. Porras, A. Dubietis, A. Piskarskas, and P. Di Trapani, Phys. Rev. Lett. **99**, 223902 (2007).
[15] O. Jedrkiewicz, M. Clerici, E. Rubino, and P. Di Trapani, Phys. Rev. A **80**, 033813 (2009).
[16] A. Couairon, E. Gaizauskas, D. Faccio, A. Dubietis, and P. Di Trapani, Phys. Rev. E **73**, 016608 (2006).
[17] M. A. Porras and P. Di Trapani, Phys. Rev. E **69**, 066606 (2004).
[18] M. Dallaire, N. McCarthy, and M. Piché, Opt. Express **17**, 18148 (2009).
[19] O. Jedrkiewicz, Y.-D. Wang, G. Valiulis, and P. Di Trapani, Opt. Express **21**, 25000 (2013).